

Transverse Beam Dynamics

B.J. Holzer

CERN, Geneva, Switzerland

Abstract

This paper gives an overview of transverse dynamics in particle accelerators with—following the emphasis of the school—special focus on transfer lines and their application for beam injection and extraction. We will restrict ourselves to a bare introduction to the basic concepts that are needed to understand the boundary conditions to be met when we are trying to transfer a beam of charged particles from one accelerator to the next.

Keywords

Accelerator physics; transverse dynamics; transfer line; injection; extraction.

1 Introduction

If we contemplate a little on the topic of this school, we get the impression that we have to treat the problem of transferring particles from one accelerator to the next, including the quite tricky business of injecting or extracting the beam into (or out of), for example, a storage ring. Now while this involves some beautiful technical concepts, such as special magnets, kickers, and septa, the overall picture is quite a bit more than just pushing a button and getting off to beddy-byes and that's it. We have to optimize the system in such a way as to get the ideal orbit position in both transverse planes (we call them x and y for the horizontal and vertical amplitudes) and we have to get the ideal corresponding angles, x' and y' . But in addition, we have to take care that the properties of the complete particle ensemble are maintained. In particular, the beam quality—we call it the *emittance* and we will talk about it in quite some detail—has to be preserved in order not to destroy the particle density distribution during the beam transfer, where fast-acting fields are applied. Unlike any other field changes in an accelerator, the injection and extraction elements are non-adiabatic; this means that their impact on the beam is *fast* and special care has to be taken.

In this sense, this paper on transverse beam dynamics, together with the accompanying papers on longitudinal dynamics, defines the background and the language for the particular courses in this school. To be very clear from the beginning: the language that we will use, concerning transverse beam dynamics, is usually applied and valid only for periodic structures; namely synchrotrons and storage rings. The problems that are studied there are typically of the form:

How do we define the orbit of the particles in an accelerator, how do we bend the particles onto a ring, and how do we manage to keep them on—or close to—a trajectory with deviations from this ideal path of only a fraction of a millimetre?

While strictly (i.e., mathematically) spoken, this language is valid for these periodic cases only, it is so powerful and elegant that we also like to use it in linear accelerators (even linear colliders, in some cases) and in transfer lines. Thus, we will use concepts that have been developed for 'periodic structures', i.e., where the situation seen by the particle repeats itself after a certain time or distance. The reason lies at the bot of the mathematics involved. Now, while this condition is easily fulfilled in a circular accelerator, namely in the case of a synchrotron, a transfer line does not have such a built-in periodicity. The particles are passing through the structure only once and that's it. However, we still like to make use of the expressions derived for the periodic machines, as they present a nifty tool for designing the accelerator as well as expressing the most relevant beam parameters. Even more, the injection and

extraction conditions have to meet the optical parameters of the connected accelerators, which are indeed periodic.

So transferring a particle beam from one accelerator to another one means the following.

- We need a system of fast-acting magnetic or electric fields that create bending forces to inject or extract the beam (or a number of bunches).
- We have to install magnetic bending fields to guide the particles in the transfer line from one place to the next.
- We have to use focusing forces (quadrupole lenses) to keep the particle ensemble close together and match the optical conditions defined by the pre- and post-accelerator at both ends of the line.
- Finally, we have to take care of the timing, i.e., the right moment of the beam transfer. We have to trigger our transfer elements in such a way that the particles, running down the transfer line, will arrive in the new machine (usually) in the centre of the new RF bucket. This last item, however, is beyond our scope here and will be treated in the following paper on longitudinal dynamics.

2 Transverse beam dynamics

The transverse beam dynamics of charged particles in an accelerator describes the movement of single particles under the influence of external transverse bending and focusing fields. It includes the detailed arrangement (for example, their positions in the machine and their strengths) of the accelerator magnets used to obtain well-defined, predictable parameters of the stored particle beam, and it describes methods to optimize the trajectories of single particles, as well as the dimensions of the beam, considered as an ensemble of many particles. A detailed treatment of this field in full mathematical detail, including sophisticated lattice optimizations, such as the right choice of the basic lattice cells and the design of dispersion suppressors or chromaticity compensation schemes, is beyond the scope of this overview. For further reading and for more detailed descriptions, we therefore refer to the more complete explanations in Refs. [1–3]. For the time being, we will just give a basic introduction to the topic and explain with—more or less hand-waving—how the trick goes.

2.1 Geometry of the ring

In general, magnetic fields are used in circular accelerators to provide the bending force and to focus the particle beam. In principle, the use of electrostatic fields would also be possible, but at high momenta (i.e., if the particle velocity is close to the speed of light), magnetic fields are much more efficient. The force acting on the particles, the Lorentz force, is given by

$$\mathbf{F} = q \cdot (\mathbf{E} + \mathbf{v} \times \mathbf{B}). \quad (1)$$

For high-energy particle beams, the velocity v is close to the speed of light and so represents a nice amplification factor whenever we apply a magnetic field. As a consequence, it is much more convenient to use magnetic fields to bend and focus the particles.

Therefore, neglecting electric fields for the moment, we write the Lorentz force and the centrifugal force on the particle on its circular path as

$$F_{\text{Lorentz}} = e \cdot v \cdot B, \quad (2)$$

$$F_{\text{centrifugal}} = \frac{\gamma m_0 v^2}{\rho}. \quad (3)$$

Assuming an idealized homogeneous dipole magnet along the particle orbit, having pure vertical field lines, we define the condition for a perfect circular orbit as equality between these two forces. This yields

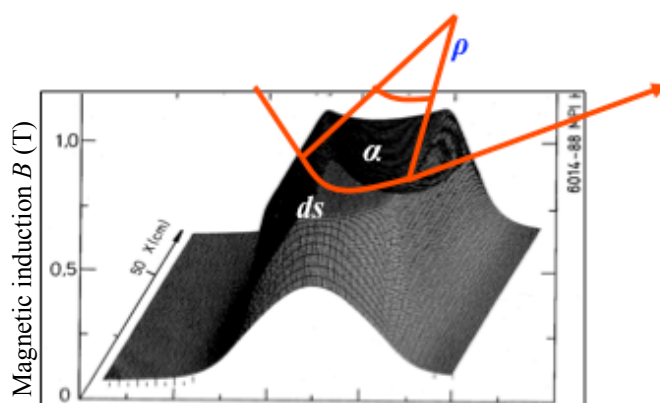


Fig. 1: Field map of a storage ring dipole magnet, and schematic path of a particle

the following condition for the idealized ring:

$$\frac{p}{e} = B \cdot \rho, \quad (4)$$

where we are referring to protons and have accordingly set $q = e$. This condition relates the so-called beam rigidity $B\rho$ to the momentum of a particle that can be carried, e.g., in a storage ring, and it ultimately defines, for a given magnetic field, the bending angle that we can achieve if a dipole field is applied to bend the beam in a transfer line or to extract it from a pre-accelerator. In reality, instead of having a continuous dipole field, the structure of our accelerator or transfer line (we call it the *lattice*) will consist of several dipole magnets, usually powered in series to define the geometry of the ring.

Now, for completeness, we would like to add two more drops of information. Clearly enough, the same argument that we used for the effect of magnetic fields is also true in the case of electrostatic fields. Again, the effect depends on the inverse of the momentum and we get e.g., for the bending angle in an electric field

$$\theta_{\text{el}} = \frac{El}{p\beta}.$$

The second comment to make here is that as soon as we talk about *low-energy* particles, it might turn out that magnetic fields are not the ideal choice. They will have a small effect on the beam as soon as the particle velocity is low. Then the accelerator components might better be electrostatic devices instead of magnets; they are also usually smaller and could be the preferred choice if the available space is limited.

Coming back to the more common situation of magnets as bending and focusing elements, we sketch the trajectory of a single particle in Fig. 1. In the free space outside the dipole magnet, the particle trajectory follows a straight line. As soon as the particle enters the magnet, it is bent onto a circular path until it leaves the magnet at the other side.

The overall effect of the main bending (or ‘dipole’) magnets in the ring is to define a more or less circular path, which we call the ‘design orbit’. By definition, this design orbit has to be a closed loop, and so the main dipole magnets in the ring have to define a full bending angle of exactly 2π . If α denotes the bending angle of a single magnet, then

$$\alpha = \frac{ds}{\rho} = \frac{B ds}{B \cdot \rho}. \quad (5)$$

We therefore require that, integrating over all dipole magnets, we get

$$\frac{\int B ds}{B \cdot \rho} = 2\pi. \quad (6)$$



Fig. 2: Superconducting dipole magnet in the LHC storage ring

Thus, a storage ring or synchrotron is not a ‘ring’ in the true sense of the word but more a polygon, where ‘poly’ means the discrete number of dipole magnets installed in the ‘ring’.

In the extreme case of the LHC, the dipole field has been pushed to the highest achievable values: 1232 superconducting dipole magnets, each 15 m long, define the geometry of the ring (or better 1232-gon, whatever the Greek expression for that might be), and, via Eq. (6), they determine the maximum momentum for the stored proton beam. Using these equations, for a maximum momentum $p = 7 \text{ TeV}/c$, we obtain a required magnetic field of

$$B = \frac{2\pi \cdot 7000 \cdot 10^9 \text{ eV}}{1232 \cdot 15 \text{ m} \cdot 2.99792 \cdot 10^8 \text{ m s}^{-1}}, \quad (7)$$

or

$$B = 8.33 \text{ T}, \quad (8)$$

to bend the beams. For convenience, we have expressed the particle momentum in units of GeV/c here. Figure 2 shows a photograph of one of the LHC dipole magnets, built with superconducting NbTi filaments, which are operated at a temperature $T = 1.9 \text{ K}$.

2.2 Focusing properties

In addition to the main bending magnets that guide the beam onto a closed orbit, focusing fields are needed to keep the particles close together. In modern storage rings and light sources, we have to keep more than 10^{12} particles in the machine, distributed over a number of bunches, and these particles have to be focused to keep their trajectories close to the design orbit. Furthermore, they are stored in the machine for many hours, and a carefully designed focusing structure is needed to maintain the necessary beam size in the ring and guarantee stability of the transverse motion.

Following classical mechanics, linear restoring forces are used, just as in the case of a harmonic pendulum. Quadrupole magnets provide the corresponding field property: they create a magnetic field that depends linearly on the amplitude of the particle, i.e., the distance of the particle from the design orbit:

$$B_x = -g \cdot y, \quad B_y = -g \cdot x. \quad (9)$$

The constant g is called the gradient of the magnetic field and it characterizes the focusing strength of the quadrupole lens in both transverse planes. The minus sign is a convention that follows the fact that for a positive amplitude, the field configuration of a focusing quadrupole will lead to a Lorentz force that reduces this amplitude, according to Fig. 3. As in the case of the dipole field, the quadrupole gradient

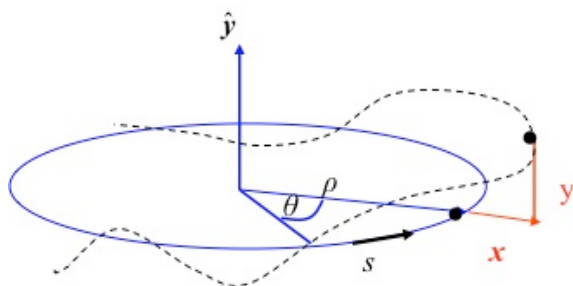


Fig. 3: Co-ordinate system used in particle beam dynamics; the longitudinal co-ordinate s moves around the ring with the particle considered.



Fig. 4: Superconducting quadrupole magnet in the LHC storage ring

is usually normalized to the particle momentum to obtain expressions that are valid for any particle momentum or energy. This normalized gradient is denoted k and defined as

$$k = \frac{g}{p/e} = \frac{g}{B\rho} . \quad (10)$$

The technical layout of such a quadrupole—again we use the LHC design as an example—is depicted in Fig. 4. As in the case of the dipoles, the LHC quadrupole magnets were built using superconducting technology to achieve the highest possible focusing forces.

Now that we have defined the two basic building blocks of a storage ring, we need to arrange them in a so-called magnet lattice and optimize the field strengths in such a way as to obtain the required beam parameters. An example to show how such a magnet lattice looks like in a real storage ring is given in Fig. 5. This photograph shows the dipole (orange) and quadrupole (red) magnets in the TSR storage ring in Heidelberg [4]. Eight dipoles are used to bend the beam into a ‘circle’, and the quadrupole lenses between them provide the focusing to keep the particles within the aperture limits of the vacuum chamber.

A general design principle of modern synchrotrons and storage rings should be pointed out here. In general, these machines are built following a so-called separate-function scheme: every magnet is designed and optimized for a certain task, such as bending, focusing, or chromatic correction. We separate the magnets in the design according to the job they are supposed to do; only in rare cases is a combined-function scheme chosen nowadays, where different magnet properties are combined in one piece of hardware. To express this principle mathematically, we use the general Taylor expansion of the normalized magnetic field,

$$\frac{B(x)}{p/e} = \frac{1}{\rho} + k \cdot x + \frac{1}{2!}mx^2 + \frac{1}{3!}nx^3 + \dots , \quad (11)$$



Fig. 5: The TSR storage ring, Heidelberg, is a typical example of a separate-function strongly focusing storage ring [4].

where $1/\rho$ refers to the normalized dipole component, k to the quadrupole contribution, and, n, m , etc., to the field contributions from the higher-order multipoles. Following these arguments, for the moment we take into account only constant (dipole) or linear (quadrupole) terms. The higher-order contributions to the field will be treated later as (hopefully) small perturbations.

Under these assumptions, we can derive—in linear approximation—the equation of motion of the transverse particle movement. We start with a general expression for the radial acceleration, known from classical mechanics (see, e.g., Ref. [5]):

$$a_r = \frac{d^2\rho}{dt^2} - \rho \left(\frac{d\theta}{dt} \right)^2 . \quad (12)$$

The first term refers to an explicit change in the bending radius, and the second to the centrifugal acceleration. Referring to our co-ordinate system, and replacing the ideal radius ρ with $\rho+x$ for the general case (Fig. 3), we obtain the relation for the balance between the radial force and the counteracting Lorentz force:

$$F = m \frac{d^2}{dt^2}(x + \rho) - \frac{mv^2}{x + \rho} = evB . \quad (13)$$

On the right-hand side of the equation, we take only linear terms of the magnetic field into account,

$$B_y = B_0 + x \frac{dB_y}{dx} , \quad (14)$$

and for convenience we replace the independent variable t with the co-ordinate s ,

$$x' = \frac{dx}{ds} = \frac{dx}{dt} \frac{dt}{ds} , \quad (15)$$

‘Convenience’ in this context means that we are more interested in the amplitude x and angle x' of the particle trajectory and therefore prefer the derivative of x with respect to s . Thus, we obtain an expression for the particle trajectories under the influence of the focusing properties of the quadrupole and dipole fields in the ring, described by a differential equation. This equation is derived in its full beauty elsewhere [3], so we shall just state it here:

$$x'' - x \cdot \left(k - \frac{1}{\rho^2} \right) = 0 , \quad (16)$$

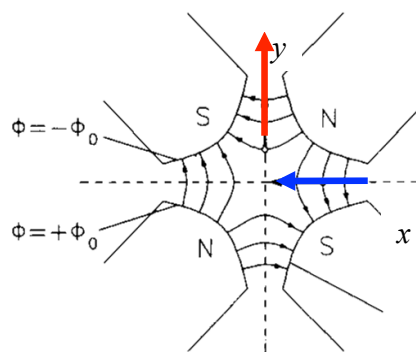


Fig. 6: Field configuration in a quadrupole magnet and the direction of the focusing and defocusing forces in the horizontal and vertical planes.

where k is the normalized gradient introduced in Eq. (11) and the $1/\rho^2$ term represents so-called weak focusing, which is a property of the bending magnets. Depending on the actual sign of k , the quadrupole will focus (negative sign) or defocus (positive sign) the beam in the corresponding plane. The particles will now follow the ‘circular’ path defined by the dipole fields and, while they are running around the machine on this path, they will, in addition, undergo harmonic oscillations in both transverse planes. The situation is shown schematically in Fig. 3. An ideal particle will follow the design orbit represented by the circle in the diagram. Any other particle will perform transverse oscillations under the influence of the external focusing fields, and the amplitude of these oscillations will ultimately define the beam size. To be brief, and referring to the horizontal plane for a moment, we can make the statement that: *‘under the influence of the focusing fields from the quadrupoles k and dipoles $1/\rho^2$, the transverse movement of the particles inside the single lattice elements looks like a harmonic oscillation’*.

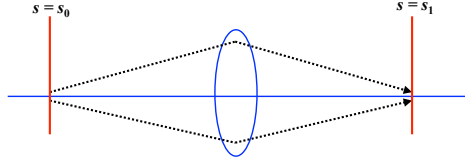
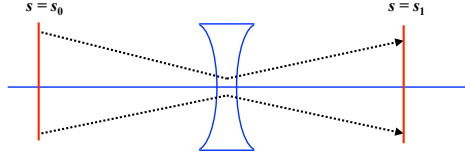
Unlike the case of a classical harmonic oscillator, however, the equations of motion in the horizontal and vertical planes differ somewhat. Assuming a horizontal focusing magnet, the equation of motion is as shown in Eq. (16). In the vertical plane, however, because of the orientation of the field lines and thus—in the end—by Maxwell’s equations, the forces instead have a defocusing effect. Also, the weak focusing term disappears in general:

$$y'' + y \cdot k = 0. \quad (17)$$

The principal problem arising from the different directions of the Lorentz force in the two transverse planes of a quadrupole field is sketched in Fig. 6. As a consequence, to overcome this uncomfortable situation, we have to explicitly introduce quadrupole lenses that focus the beam in the horizontal and vertical directions in some alternating order. It is the task of the machine designer to find an adequate solution to this problem and to define a magnet pattern that will provide an overall focusing effect in both transverse planes. The rest is easy, in the sense of A. Wolski’s statement: “. . . in principle, there are only two steps in the analysis of any dynamical system. The first step is to write down the equations of motion; and the second step is to solve them” [6].

Now, following closely the example of the classical harmonic oscillator, we can write down the solutions of the equations of motion. For simplicity, we focus on the horizontal plane; a ‘focusing’ magnet is therefore focusing in this horizontal plane and at the same time defocusing in the vertical plane. Starting with the initial conditions for the particle amplitude x_0 and angle x'_0 in front of the magnet element, we obtain the following relations for the trajectory inside the magnet:

$$x(s) = x_0 \cdot \cos\left(\sqrt{|K|} s\right) + x'_0 \cdot \frac{1}{\sqrt{|K|}} \sin\left(\sqrt{|K|} s\right), \quad (18)$$


Fig. 7: Effect of a focusing quadrupole magnet

Fig. 8: Effect of a defocusing quadrupole magnet

$$x'(s) = -x_0 \cdot \sqrt{|K|} \sin(\sqrt{|K|} s) + x'_0 \cdot \cos(\sqrt{|K|} s). \quad (19)$$

Here, the parameter K combines the quadrupole gradient and the weak focusing effect: $K := 1/\rho^2 - k$. Usually, these two equations are combined into a more elegant and convenient matrix form,

$$\begin{pmatrix} x \\ x' \end{pmatrix}_s = \mathbf{M}_{\text{foc}} \begin{pmatrix} x \\ x' \end{pmatrix}_0, \quad (20)$$

where the matrix \mathbf{M}_{foc} contains all the relevant information about the magnet element:

$$\mathbf{M}_{\text{foc}} = \begin{pmatrix} \cos(\sqrt{|K|} s) & \frac{1}{\sqrt{|K|}} \sin(\sqrt{|K|} s) \\ -\sqrt{|K|} \sin(\sqrt{|K|} s) & \cos(\sqrt{|K|} s) \end{pmatrix}. \quad (21)$$

The situation is illustrated in Fig. 7.

In the case of a defocusing magnet (or to be quite clear, also, in the case of the vertical plane, of a horizontal focusing magnet), we obtain analogously that

$$\begin{pmatrix} x \\ x' \end{pmatrix}_s = \mathbf{M}_{\text{defoc}} \begin{pmatrix} x \\ x' \end{pmatrix}_0, \quad (22)$$

with

$$\mathbf{M}_{\text{defoc}} = \begin{pmatrix} \cosh(\sqrt{|K|} s) & \frac{1}{\sqrt{|K|}} \sinh(\sqrt{|K|} s) \\ \sqrt{|K|} \sinh(\sqrt{|K|} s) & \cosh(\sqrt{|K|} s) \end{pmatrix}; \quad (23)$$

see Fig. 8.

For completeness, we also include the case of a field-free drift. With $K = 0$, we obtain

$$\mathbf{M}_{\text{drift}} = \begin{pmatrix} 1 & s \\ 0 & 1 \end{pmatrix}. \quad (24)$$

This matrix formalism allows us to combine the elements of a storage ring in an elegant way, and so it is straightforward to calculate particle trajectories. In this context, we would like to emphasize a few points:

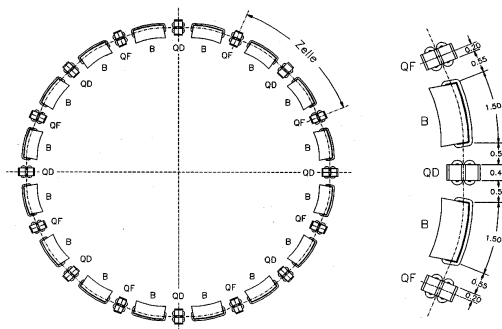


Fig. 9: Simple periodic chain of bending magnets (B) and focusing (QF) or defocusing (QD) quadrupoles forming the basic structure of a storage ring. Courtesy, K. Wille [1].

- a certain quadrupole lens will always have two opposing effects: focusing in one plane and defocusing in the other;
- et vice versa (*‘and the other way round’*, for the non-Latin-speaking community);
- we therefore like to combine these effects in a common 4×4 matrix’;
- in linear approximation and without explicit coupling fields, such as roll angles of the quadrupoles or solenoids, the motion in the two transverse planes is uncoupled. An amplitude in the horizontal direction, e.g., will not have any influence on the vertical motion and therefore the corresponding non-diagonal elements of the matrix $M_{1,3}$, $M_{1,4}$, etc., are zero.

It is therefore convenient to describe this simultaneous effect in the two planes in a single 4×4 matrix and define a vector for both transverse amplitudes and angles:

$$\begin{pmatrix} x \\ x' \\ y \\ y' \end{pmatrix}_s = \begin{pmatrix} \cos(\sqrt{|K|}s) & \frac{1}{\sqrt{|K|}} \sin(\sqrt{|K|}s) & 0 & 0 \\ -\sqrt{|K|} \sin(\sqrt{|K|}s) & \cos(\sqrt{|K|}s) & 0 & 0 \\ 0 & 0 & \cosh(\sqrt{|K|}s) & \frac{1}{\sqrt{|K|}} \sinh(\sqrt{|K|}s) \\ 0 & 0 & \sqrt{|K|} \sinh(\sqrt{|K|}s) & \cosh(\sqrt{|K|}s) \end{pmatrix} \cdot \begin{pmatrix} x \\ x' \\ y \\ y' \end{pmatrix} \quad (25)$$

As an example of a larger structure, we consider the simple case of an alternating focusing and defocusing lattice, a so-called FODO lattice, see Fig. 9.

As we know the properties of each and every element in the accelerator, we can construct the corresponding matrices and calculate, step by step, the amplitude and angle of a single-particle trajectory around the ring. Even more conveniently, we can multiply out the different matrices and, given initial conditions x_0 and x'_0 at a certain position in the storage ring, obtain directly the trajectory at any location in the ring:

$$\mathbf{M}_{\text{total}} = \mathbf{M}_{\text{foc}} \cdot \mathbf{M}_{\text{drift}} \cdot \mathbf{M}_{\text{dipole}} \cdot \mathbf{M}_{\text{drift}} \cdot \mathbf{M}_{\text{defoc}} \cdots \quad (26)$$

The trajectory thus obtained is shown schematically in Fig. 10.

We have to point out the following facts in this context.

- At each moment, which means inside each lattice element, the trajectory is part of a harmonic oscillation.
- However, because of the different restoring or defocusing forces, the solution will look different at each location.
- In the linear approximation that we have used in this context, all particles experience the same external fields, and their trajectories will differ only because of their different initial conditions.

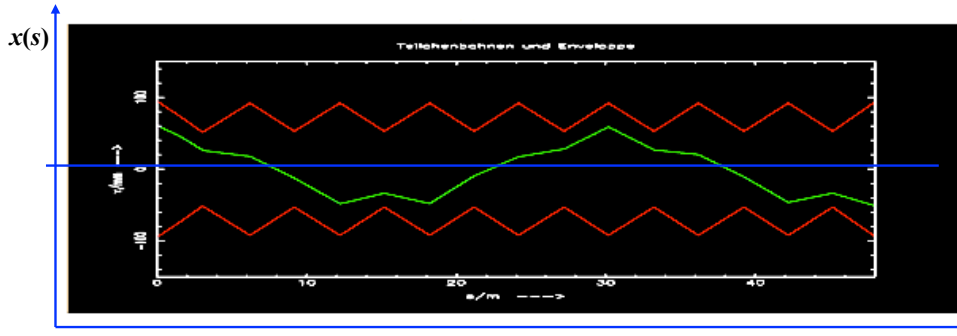


Fig. 10: Calculated particle trajectory in a simple storage ring

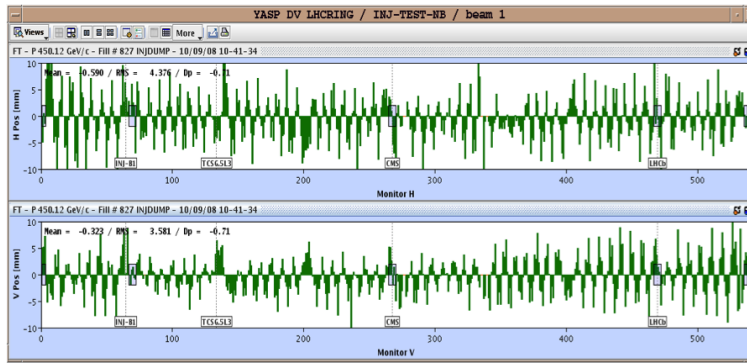


Fig. 11: Beam position measured at the injection septum and after the first turn around the machine during one of the very first beam injections into the LHC storage ring.

- There seems to be an overall oscillation in both transverse planes while the particle is travelling around the ring. Its amplitude stays well within the boundaries set by the vacuum chamber, and its frequency in the example of Fig. 10 is roughly 1.4 transverse oscillations per revolution, which corresponds to the eigenfrequency of the particle under the influence of the external fields.

Coming closer to a real, existing machine, Fig. 11 shows an orbit, measured during one of the first injections into the LHC storage ring. The horizontal oscillations are plotted in the upper half of the figure and the vertical oscillations in the lower half, on a scale of ± 10 mm. Each histogram bar indicates the value recorded during the first turn of the beam by a beam position monitor at a certain location in the ring; the orbit oscillations are clearly visible. During these first injections, a beam screen had been introduced right after the injection point. In Fig. 12, the spot of the injected beam is clearly visible as well as the one after the first turn. In both transverse planes, these spots are not yet lying on top of each other and so the orbit is not yet closed. Here we have to emphasize very clearly that until this moment the storage ring ‘LHC’ is a simple transfer line. The conditions of horizontal and vertical orbit amplitude at the injection point and after one turn are not the same. While this seems to have a small effect on the orbit, it makes a large difference in the mathematical treatment and for the matter of resonances that can amplify orbit fluctuations. We will come back to this problem in a later section. However, in the case of Fig. 12, after a straightforward orbit correction, the closed orbit condition can be achieved and we finally obtain what we call a ‘stored beam’.

By counting (or, better, fitting) the number of oscillations in both transverse planes, we obtain, in the case of the LHC, values of

$$Q_x = 64.31, \quad Q_y = 59.32. \quad (27)$$

TRANSVERSE BEAM DYNAMICS

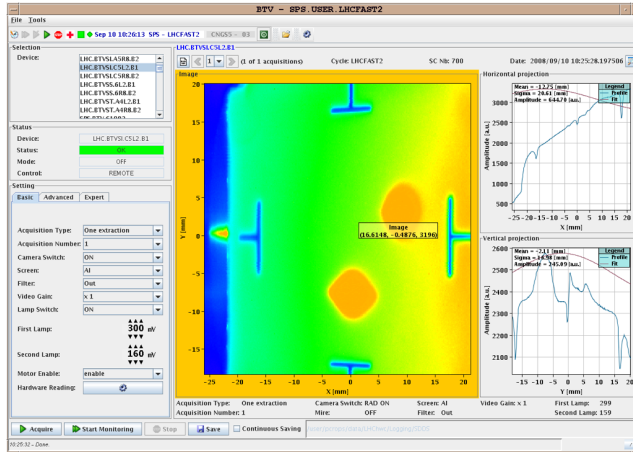


Fig. 12: Measured orbit of the first turn in LHC during the commissioning of the machine. The beam screen is located immediately after the injection septum and shows the spot at injection and after one full turn around the machine.



Fig. 13: Tune signal of proton beam in storage ring (HERA-p)

These values, which describe the eigenfrequencies of the particles, are called the horizontal and vertical *tunes*, respectively. Knowing the revolution frequency, we can easily calculate the transverse oscillation frequencies, which correspond to these tune values and which, for this type of machine, usually lie in the range of some hundreds of kilohertz.

As the tune characterizes the particle oscillations under the influence of all external fields, it is one of the most important parameters of a storage ring. Therefore, it is usually displayed and controlled at all times by the control system of such a machine. As an example, Fig. 13 shows the tune diagram of the HERA proton ring [7]; this was obtained via a Fourier analysis of a spectrum measured from the signal of the complete particle ensemble. The peaks indicate the two tunes in the horizontal and vertical planes of the machine; in a sufficiently linear machine, a fairly narrow spectrum is obtained.

Briefly referring back to Fig. 10, the question is what the trajectory of the particle will look like in the second turn, or the third, or after an arbitrary number of turns. Now, as we are dealing with a circular machine, the amplitude x and angle x' at the end of the first turn will be the initial conditions for the second turn, and so on. After many turns, the overlapping trajectories begin to form a pattern, such as that shown in Fig. 14, which indeed looks like a beam that here and there has a larger or a smaller size but still remains well-defined in its amplitude by the external focusing forces.

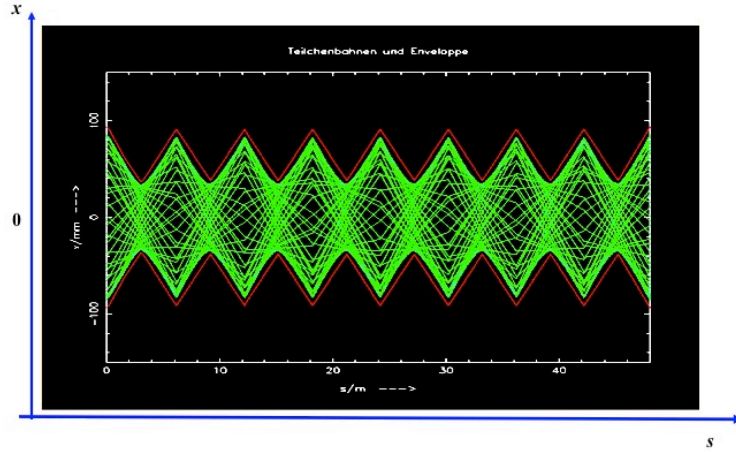


Fig. 14: Many single-particle trajectories together form a pattern that corresponds to the beam size in the ring

3 The Twiss parameters α , β , and γ

As explained in the last section, repeating the calculations that led to the orbit of the first turn will result in a large number of single-particle trajectories that overlap in some way and form the beam envelope. Figure 14 shows the result for 50 turns. Clearly, as soon as we are talking about many turns or many particles, the use of the single-trajectory approach is quite limited and we need a description of the beam as an ensemble of many particles. Fortunately, in the case of periodic conditions in the accelerator, there is another way to describe the particle trajectories and, in many cases, it is more convenient than the aforementioned formalism. It is important to note that, in a circular accelerator, the focusing elements are necessarily periodic in the orbit co-ordinate s after one revolution. Furthermore, storage ring lattices have an internal periodicity in most cases: they are often constructed, at least partly, from sequences in which identical magnetic structures, the lattice cells, are repeated several times in the ring and lead to periodically repeated focusing properties. In this case, the equation of motion can now be written in a slightly different form:

$$x''(s) - k(s) \cdot x(s) = 0, \quad (28)$$

where, for simplicity, we refer to a pure quadrupole magnet and so the $1/\rho^2$ term does not appear. The main issue, however, is that unlike the previous treatment, the focusing parameters (or restoring forces) are no longer constant but are functions of the co-ordinate s . However, they are periodic in the sense that, at least after one full turn, they repeat themselves, i.e., $k(s + L) = k(s)$, leading to the so-called Hill differential equation (28). Following Floquet's theorem [2], the solution of this equation can be written in its general form as

$$x(s) = \sqrt{\varepsilon} \sqrt{\beta(s)} \cos(\psi(s) - \phi), \quad (29)$$

where ψ is the phase of the oscillation, ϕ is its initial condition, and ε is a characteristic parameter of a single particle or, if we are considering a complete beam, of the ensemble of particles. Taking the derivative with respect to s , we get the trajectory angle x' :

$$x'(s) = \sqrt{\varepsilon} \sqrt{\beta(s)} \left(\frac{1}{2} \beta'(s) \cos(\psi(s) - \phi) + \sin(\psi(s)) \right). \quad (30)$$

The position and angle of the transverse oscillation of a particle at a point s are given by the value of a special amplitude function, the β -function, at that location; ε and ϕ are constants of any particular trajectory. The β -function depends in a rather complicated manner on the overall focusing properties of the storage ring. It cannot be calculated directly by an analytical approach, but instead must be either

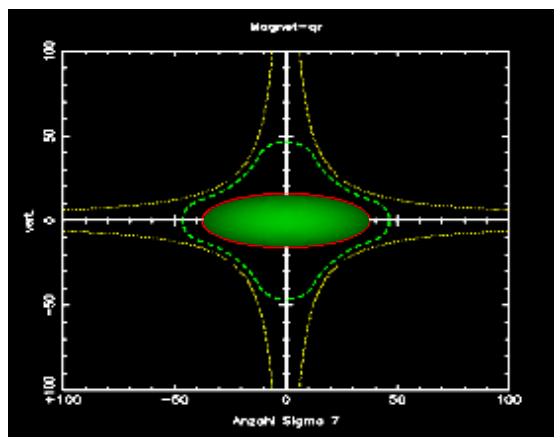


Fig. 15: Transverse beam shape inside a quadrupole magnet: plotted are 7σ of a Gaussian particle density distribution inside the vacuum chamber and magnet aperture.

determined numerically or deduced from properties of the single-element matrices (see, e.g., Ref. [3]). In any case, like the lattice itself, it has to fulfil the periodicity condition

$$\beta(s + L) = \beta(s). \quad (31)$$

Inserting the solution (Eq. (29)) into the Hill equation and rearranging slightly, we get

$$\psi(s) = \int_0^s \frac{ds}{\beta(s)}, \quad (32)$$

which describes the phase advance of the oscillation. It should be emphasized that ψ depends on the particle's oscillation amplitude. At locations where β reaches large values, i.e., the beam has a large transverse dimension, the corresponding phase advance is small; conversely, at locations where we create a small β in the lattice, we obtain a large phase advance. In the context of Fig. 10, we introduced the tune as the number of oscillations per turn, which is nothing other than the overall phase advance of the transverse oscillation per revolution in units of 2π . So, by integrating Eq. (32) around the ring, we get for the tune, the expression

$$Q = \frac{1}{2\pi} \oint \frac{ds}{\beta(s)}. \quad (33)$$

The practical significance of the β -function is shown in Figs. 14 and 15. Whereas in Fig. 14 the single-particle trajectories are plotted turn by turn, Fig. 15 shows schematically a section through the transverse shape of the beam and indicates the beam size inside the vacuum chamber. The hyperbolic profile of the pole shoes of the quadrupole lens is sketched as a yellow dashed line, and the envelope of the overlapping trajectories, given by $\hat{x} = \sqrt{\varepsilon\beta(s)}$, is marked in red and used to define the beam size in the sense of a Gaussian density distribution.

3.1 β , ε , and the phase space ellipses

Although the β -function is a somewhat abstract parameter that results from all focusing and defocusing elements in the ring, the integration constant ε has a well-defined physical interpretation. Given the solution of Hill's equation, Eq. (29), and its derivative, Eq. (30), we can transform the first equation to

$$\cos(\psi(s)) = \frac{x(s)}{\sqrt{\varepsilon\beta(s)}} \quad (34)$$

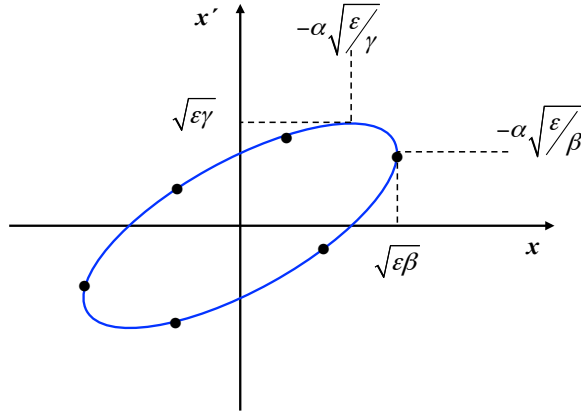


Fig. 16: Ellipse in (x, x') phase space

and insert the expression into Eq. (30) to get an expression for the integration constant ε :

$$\varepsilon = \gamma(s)x^2(s) + 2\alpha x(s)x'(s) + \beta(s)x'^2(s). \quad (35)$$

Here we have followed the usual convention in the literature and introduced the two parameters

$$\alpha(s) = -\frac{1}{2}\beta'(s) \quad (36)$$

and

$$\gamma(s) = \frac{1 + \alpha^2(s)}{\beta(s)}. \quad (37)$$

On having a closer look at Eq. (35), we realize that we obtain for ε a parametric representation of an ellipse in the (x, x') ‘phase space’. Now the mathematical integration constant ε gains physical meaning. In fact, ε describes the space occupied by the particle in the transverse (x, x') phase space (simplified here to a two-dimensional space). More specifically, the area in the (x, x') space that is covered by the particle is given by

$$A = \pi \cdot \varepsilon, \quad (38)$$

and, as long as we consider only conservative forces acting on the particle, this area is constant according to Liouville’s theorem. Here, we take these facts as given, but we should point out that, as a direct consequence, the so-called emittance ε cannot be influenced by any external fields; it is a property of the beam, and we have to take it as given and act with caution in order not to dilute it.

Here a little side remark is appropriate—at least for the theoretical purists: the real phase space, as we know it from classical mechanics, refers to the canonical conjugate variables, x and p_x . In beam dynamics, however, we keep it a bit simpler and draw the dynamics of our particles in an x – x' co-ordinate system. To point out the difference and to make things clear, sometimes the x – x' space is therefore called the ‘trace-space’. However this expression is not (yet) fully accepted in the literature. Still, there are some remarkable consequences; we will come back to this point in the next section.

To be more descriptive, and following the usual textbook treatment of accelerators, we can draw the ellipse of the particle’s transverse motion in phase space; see, for example, Fig. 16. The shape and orientation of the ellipse are determined by the optics function β and its derivative, $\alpha = -\frac{1}{2}\beta'$, and so change as a function of the position s in the ring; the area covered in phase space, however, is constant throughout the machine.

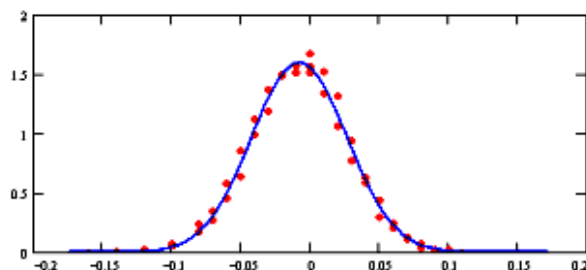


Fig. 17: Transverse particle distribution in a storage ring. The dots correspond to the measurement; the line is a Gaussian fit. A particle at 1σ from the beam centre is used to represent the beam size.

In Fig. 16, expressions for the dependence of the beam size and divergence and, as a consequence, the shape and orientation of the phase space ellipse are included. For the sake of simplicity, we shall not derive these expressions here; instead, see Ref. [3].

Referring once more to the issue of beam injection, it is clear now that in order to obtain a perfect beam transfer into a storage ring, it is *not* sufficient to correct the orbit, which means to get the origin of the phase space ellipse right. In addition, we have to optimize the beam optics of the transfer line in such a way that at the end we obtain the optics functions α and β that correspond to the lattice of the ring. Only then will a dilution of the emittance be avoided. This is valid for both transverse planes.

To complete the picture, we are now plotting, for a given position s in the ring, the co-ordinates x and x' of a single particle, turn by turn; doing so, we obtain the phase space co-ordinates of the particle, as shown in Fig. 16 (marked as dots in the figure). These co-ordinates follow the form of the ellipse, and the particle performs, from one turn to the next, a number of revolutions in phase space that corresponds to its tune. We have already emphasized that, as long as only conservative forces are considered (i.e., no interaction between the particles in a bunch, no collisions with remaining gas molecules, no radiation effects, etc.), the size of the ellipse in (x, x') space is constant and can be considered a quality factor of a single particle. Large areas in (x, x') space mean large amplitudes and angles of the transverse particle motion, and we would consider this as meaning a low particle ‘quality’.

Finally, let us now talk a little more about the beam as an ensemble of many (typically 10^{11}) particles. Referring to Eq. (29), at a given position in the ring, the beam size is defined by the emittance ε and the amplitude function β . Thus, at a certain moment in time, the cosine term in Eq. (29) will be equal to one and the amplitude of the trajectory will reach its maximum value. Now, if we consider a particle at one standard deviation (σ) of the transverse density distribution, then by using the emittance of this reference particle we can calculate the size of the complete beam, in the sense that the complete area (within one sigma) of all particles in the (x, x') phase space is surrounded (and so defined) by our one-sigma candidate. Thus, the value $\sqrt{\varepsilon \cdot \beta(s)}$ defines the one-sigma beam size in the transverse plane.

An example of such a particle density distribution is shown in Fig. 17. The dots correspond to the measured values of the particle distribution at the collision point and the blue curve represents a Gaussian fit. The emittance (usually referred to as ‘Courant–Snyder invariant’) of the single particle at 1σ from the centre is used as representative of the emittance of the complete beam ensemble.

It is the task of the lattice designer to establish beam optics that guarantee—for a given beam emittance—values of the β -function that lead to tolerable beam sizes at every location in the machine. As an example, we shall use the values for the LHC proton beam (Fig. 18). In the periodic pattern of the arc, the β -function is equal to 180 m and the emittance ε at the flat-top energy is roughly 5×10^{-10} rad m. The resulting typical beam size is, therefore, 0.3 mm. Now, clearly, we would not design a vacuum aperture for the machine based on a one-sigma beam size; typically, an aperture requirement corresponding to 12σ is a good rule to guarantee a sufficient beam lifetime, allowing for tolerances arising from magnet

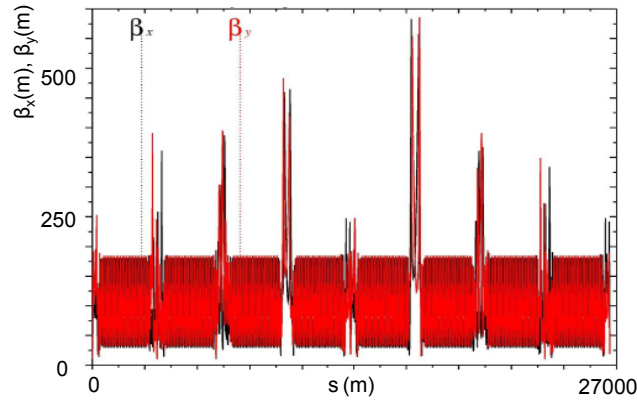


Fig. 18: LHC beam optics at injection energy: owing to the larger beam emittance at low energy, the beta-function has to be limited to values of about 600 m in the straight sections, while in the arc the periodic solution reaches a level of about 180 m.

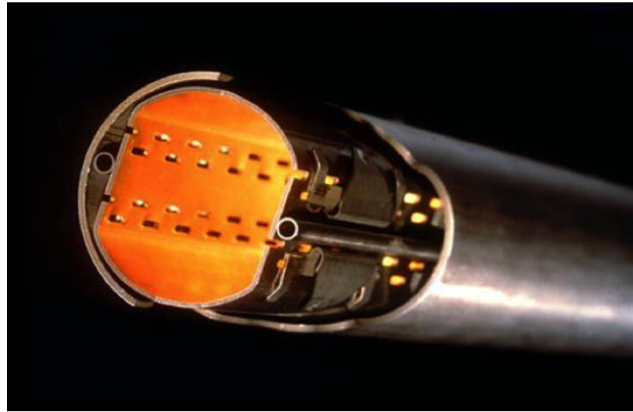


Fig. 19: LHC vacuum chamber with beam screen to shield the bore of the superconducting magnet from synchrotron radiation.

misalignment, optics errors, orbit fluctuations, and operational flexibility. In Fig. 19, part of the LHC vacuum chamber is shown, including the beam screen used to protect the cold bore from synchrotron radiation; its aperture limit corresponds to at least 18σ of the beam size.

3.2 Adiabatic shrinking

The definition of the beam emittance described in the previous section bears a certain problem. Strictly speaking, Liouville's theorem states that—given conservative forces—the particle density in the phase space x, p_x is constant. Now in accelerator physics we are talking about particle amplitudes and angles, x, x' ; in the literature, such a co-ordinate system, defined by these variables, is sometimes called the *trace space* to make a clear distinction from the *phase space* of classical mechanics.

The main issue and important consequence for us is related to the particle acceleration. The angle x' of a particle is given by the ratio between longitudinal and transverse momentum:

$$x' = \frac{dx}{ds} = \frac{dx}{dt} \frac{dt}{ds} = \frac{p_x}{p_s} \propto \frac{1}{m_0 c \beta \gamma}, \quad (39)$$

where we express the relativistic momentum as a function of the rest mass m_0 , the relativistic parameter $\beta = v/c$ and the Lorentz factor $\gamma = 1/(\sqrt{1 - \beta^2})$. Here we have to pause for a moment and ask the

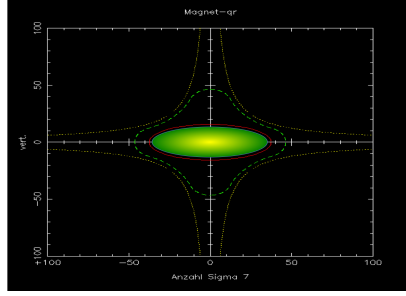


Fig. 20: Beam envelope of HERA proton ring at 40 GeV injection energy. The plot refers to 7σ at the mini-beta quadrupoles.

reader to accept our apologies. There is something called an amplitude- or β -function in beam dynamics, and now suddenly we have in addition the relative speed of the particle v/c , which is also called β . We hope that there is not too much confusion and in the end . . . it is not our fault, as it was invented by our colleagues Albert and Ernest [8]. And we can understand their trouble in finding an adequate letter, as the Greek alphabet has only three letters anyway.

Back to our problem: p_s describes the longitudinal component of the particle's momentum; it is this longitudinal component that increases during the acceleration. Now, Liouville's theorem states that, for the canonical conjugate variables x and p_x , the phase space area is constant:

$$\int p_x dx = \text{constant} \quad (40)$$

and we will not argue about that.

However, in the rather sloppy interpretation that we have used until now, we refer to a co-ordinate system x, x' and so in reality we get

$$\int x' dx = \frac{\int p_x}{p_s} dx \quad (41)$$

and as, during acceleration, the longitudinal momentum is obviously increasing, our x - x' ellipse will shrink proportionally to $1/\beta\gamma$. We conclude, therefore, that the beam emittance and, as a consequence, the beam dimension in both transverse planes will shrink during acceleration and this is indeed what we observe. As a consequence, a proton beam in a synchrotron or any particle beam in a linac will have the largest emittance at injection energy and it is here, where the beam optics—expressed as the beta-function—will have to be optimized for sufficient free aperture. The effect can be quite impressive: in Fig. 20, the 7σ envelope of a proton beam is shown inside the vacuum chamber (dashed line) of a mini-beta quadrupole magnet. The figure shows the situation at 40 GeV injection energy. In Fig. 21, for the same beam optics, and at the same location again, the 7σ envelope is shown, but now at a flat-top energy of 920 GeV. Owing to the much higher energy, the beam size is smaller by a factor of $\sqrt{920/40} = \sqrt{23}$ and the beam lifetime was considerably increased on the energy ramp of this machine.

As a direct consequence, we conclude that beam optics that lead to large beta-functions in the ring only can be applied at highest energy, where, owing to the reduced emittance, the overall beam size will still be limited. As an example, we refer again to the LHC situation. In direct comparison with the low-energy optics shown in Fig. 18, we now present the optics that are applied for high-energy collisions, in Fig. 22. Here, we can afford values of β of up to 4.5 km.

The design of the injection and extraction elements (kickers and septa), as well as the magnets for the transfer line in between, will therefore strongly depend on the beam energy considered; not only because of the trivial effect of the beam rigidity, discussed here, but also because of the emittance that determines the beam size and thus the aperture need of the injection and extraction elements.

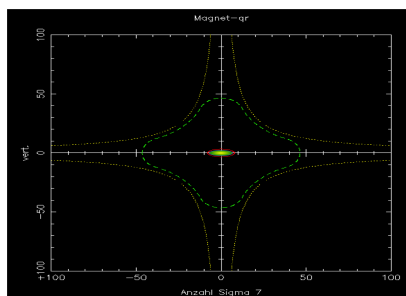


Fig. 21: Beam envelope of HERA proton ring at 920 GeV flat-top energy. The location and number of σ correspond to Fig. 20.

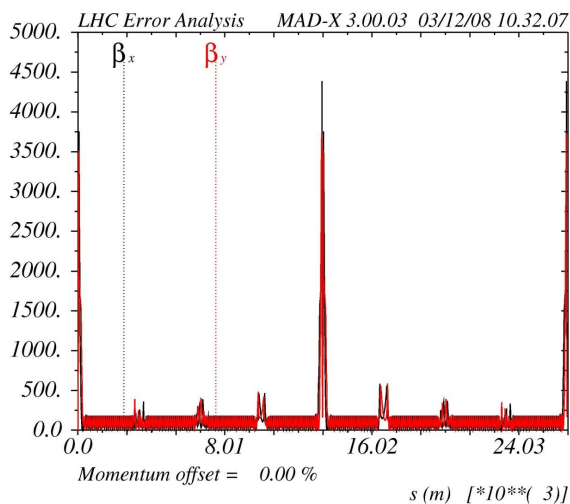


Fig. 22: LHC beam optics at high energy: owing to the small beam emittance at high energy, large values of the amplitude function β can be accepted; compare with the situation at injection energy, shown in Fig.18.

For completeness, we have to mention that as soon as synchrotron light effects must be considered, the situation changes drastically. In electron synchrotrons, the beam dynamics is determined by the equilibrium between synchrotron radiation damping and excitation due to the emitted photon quanta. Therefore, we observe a completely different behaviour; namely, a quadratic increase of the emittance with energy, $\varepsilon \propto \gamma^2$. We will summarize these facts in a later paper in this course.

4 Dispersion

So far, we have treated the beam and the equation of motion as a mono-energetic problem. Unfortunately, life is not so easy, and in the case of a real beam we have to deal with a considerable distribution of the particles with respect to energy or momentum. A typical value is

$$\frac{\Delta p}{p} \approx 1.0 \cdot 10^{-3}. \quad (42)$$

This momentum spread leads to several effects concerning the bending of the dipole magnets and the focusing strength of the quadrupoles. It turns out that the equation of motion, which has been a homogeneous differential equation until now, acquires a non-vanishing term on the right-hand side.

4.1 Dispersive effects

Replacing the ideal momentum p in Eq. (10) with $p_0 + \Delta p$, we obtain in approximation of small Δp , instead of Eq. (16):

$$x'' + x \cdot \left(\frac{1}{\rho^2} - k \right) = \frac{\Delta p}{p} \cdot \frac{1}{\rho}. \quad (43)$$

The general solution of our now inhomogeneous differential equation is, therefore, the sum of the solution of the homogeneous equation of motion and a particular solution of the inhomogeneous equation:

$$x(s) = x_\beta(s) + x_i(s). \quad (44)$$

Here, x_β is the solution that we have discussed up to now (the index β reminds us that these so-called betatron oscillations were observed for the first time in a machine called a *betatron*) and x_i is an additional contribution that still has to be determined. For convenience, we usually normalize this second term and define a special function, the so-called dispersion:

$$D(s) = \frac{x_i(s)}{\Delta p/p}. \quad (45)$$

It describes the dependence of the additional amplitude of the transverse oscillation on the momentum error of the particle. It clearly fulfils the condition

$$x_i''(s) + K(s) \cdot x_i(s) = \frac{1}{\rho} \cdot \frac{\Delta p}{p}. \quad (46)$$

As before, we have combined the weak and strong focusing effects in the parameter $K := (1/\rho^2) - k$. The dispersion function is defined by the magnet lattice and is usually calculated by optics programs in the context of the calculation of the usual optical parameters. Analytically, it can be determined for single elements via the expression

$$D(s) = S(s) \cdot \int \frac{1}{\rho(\bar{s})} C(\bar{s}) d\bar{s} - C(s) \cdot \int \frac{1}{\rho(\bar{s})} S(\bar{s}) d\bar{s}, \quad (47)$$

where $S(s)$ and $C(s)$ correspond to the sine-like and cosine-like elements of the single-element matrices or of the corresponding product matrix if several elements are considered in the lattice.

Although this all sounds somewhat theoretical, we would like to stress that typical values for the beam size and dispersive effect in the case of a high-energy storage ring are

$$x_\beta \approx 1\text{--}2 \text{ mm}, \quad D(s) \approx 1\text{--}2 \text{ m}. \quad (48)$$

Thus, for a typical momentum spread of $\Delta p/p = 1 \cdot 10^{-3}$, we obtain an additional contribution to the beam size from the dispersion function that is of the same order as that from the betatron oscillations, x_β . An example of a high-energy beam optics system including the dispersion function is shown in Fig. 23. It should be pointed out that the dispersion describes the special orbit that an ideal particle would have in the absence of betatron oscillations ($x_\beta = x'_\beta = 0$) for a momentum deviation of $\Delta p/p = 1$. In any case, it describes ‘just another particle orbit’ and so it is subject to the focusing forces of the lattice elements, as seen in the figure.

5 Transformation of the Twiss parameters α, β, γ

“Once more unto the breach, dear friends,” [9].

While it is straightforward to develop the rules for the transformation of the trajectory amplitudes and angles, (x, x') , via the single-element matrices of the lattice elements (Eq. (25)), a similar formulation

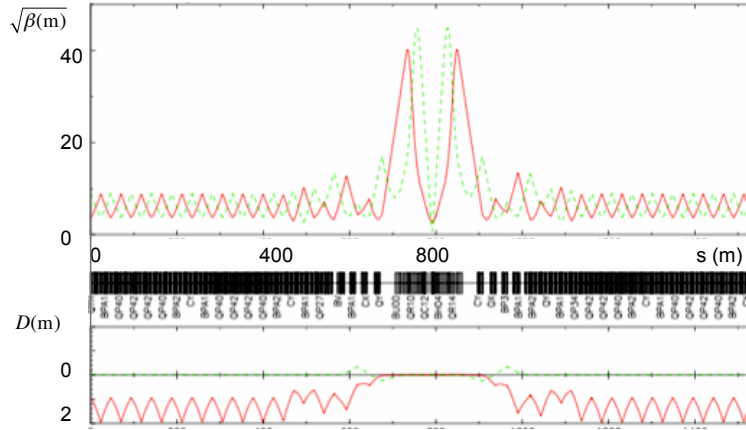


Fig. 23: β -function (top) and dispersion (bottom) of typical high-energy collider ring

can be deduced for the optical functions, α , β , and γ . The derivation is closely related to the fact that—for a given energy—the beam emittance ε is constant.

We are starting again from the usual transformation of a trajectory amplitude and angle between two locations in the lattice

$$\begin{pmatrix} x \\ x' \end{pmatrix}_{s_2} = \mathbf{M} \begin{pmatrix} x \\ x' \end{pmatrix}_{s_1}, \quad (49)$$

where the matrix \mathbf{M} describes the focusing properties of a single lattice element, or in the case of several lattice elements, it represents the product matrix, as described in Eq. (26). In the general case of a sequence of lattice elements, we write

$$\mathbf{M} = \begin{pmatrix} C & S \\ C' & S' \end{pmatrix}, \quad (50)$$

where the matrix elements C, S, \dots refer to the elements of the product matrix or, in the trivial case, of, e.g., a single focusing quadrupole, are the usual descriptions that we introduced before:

$$\mathbf{M}_{\text{foc}} = \begin{pmatrix} C & S \\ C' & S' \end{pmatrix} = \begin{pmatrix} \cos(\sqrt{|K|}s) & \frac{1}{\sqrt{|K|}} \sin(\sqrt{|K|}s) \\ -\sqrt{|K|} \sin(\sqrt{|K|}s) & \cos(\sqrt{|K|}s) \end{pmatrix}. \quad (51)$$

Now we consider two locations, s_1 and s_2 , in the storage ring, as shown schematically in Fig. 24. At both positions, the emittance can be expressed as a function of the Twiss parameters at these positions:

$$\varepsilon = \gamma_1 x^2(s_1) + 2\alpha_1 x(s_1)x'(s_1) + \beta_1 x'^2(s_1), \quad (52)$$

$$\varepsilon = \gamma_2 x^2(s_2) + 2\alpha_2 x(s_2)x'(s_2) + \beta_2 x'^2(s_2), \quad (53)$$

keeping in mind that the numerical value of the emittance at both positions has to be the same, as long as Mr. Liouville's theorem is fulfilled.

Knowing the amplitude and angle of the trajectory at position s_2 , we can deduce these values at position s_1 :

$$\begin{pmatrix} x \\ x' \end{pmatrix}_{s_1} = \mathbf{M}^{-1} \begin{pmatrix} x \\ x' \end{pmatrix}_{s_2}, \quad (54)$$

where the matrix from s_2 to s_1 is the inverse transformation matrix,

$$\mathbf{M}^{-1} = \begin{pmatrix} S' & -S \\ -C' & C \end{pmatrix} \quad (55)$$

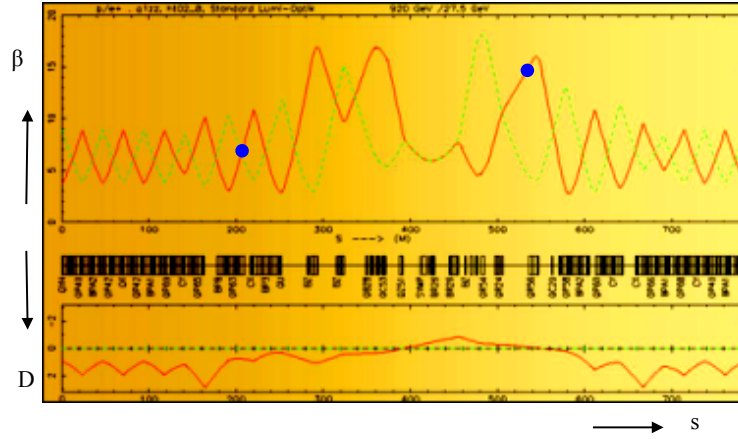


Fig. 24: The optical functions at two positions in a ring are related to each other via the constant beam emittance

and we used the fact that, for all matrices in a storage ring, the determinant has to be equal to one:

$$\text{Det}(M) = CS' - SC' = 1 . \quad (56)$$

Thus, we can write for our trajectory co-ordinates:

$$x_1 = S'x_2 - Sx_2' , \quad (57)$$

$$x_1' = -C'x_2 + Cx_2' . \quad (58)$$

Inserting these into Eq. (53), we express the emittance at position s_1 as a function of the trajectory co-ordinates at position s_2 :

$$\varepsilon = \beta_1(Cx_2' - C'x_2)^2 + 2\alpha_1(S'x_2 - Sx_2')(Cx_2' - C'x_2) + \gamma_1(S'x_2 - Sx_2')^2 . \quad (59)$$

Sorting via x and x' and comparing the coefficients, we can finally relate the Twiss functions between the two locations in the ring:

$$\begin{aligned} \beta(s_2) &= C^2\beta(s_1) - 2SC\alpha(s_1) + S^2\gamma(s_1) , \\ \alpha(s_2) &= -CC'\beta(s_1) + (SC' + S'C)\alpha(s_1) - SS'\gamma(s_1) , \\ \gamma(s_2) &= C'^2\beta(s_1) - 2S'C'\alpha(s_1) + S'^2\gamma(s_1) . \end{aligned} \quad (60)$$

Once more—for the sake of elegance in our notation—we prefer to combine these relations in matrix form and get

$$\begin{pmatrix} \beta \\ \alpha \\ \gamma \end{pmatrix}_{s_2} = \begin{pmatrix} C^2 & -2SC & S^2 \\ -CC' & SC' + S'C & -SS' \\ C'^2 & -2S'C' & S'^2 \end{pmatrix} \cdot \begin{pmatrix} \beta \\ \alpha \\ \gamma \end{pmatrix}_{s_1} . \quad (61)$$

So if we once know, by calculation or measurement, the optical functions at one position in the ring, we can determine them via the single-element matrices in the lattice at any other location. This statement holds equally for rings and for transfer lines.

However—and here we have to be careful—there is something special for transfer lines and linear accelerators that we have to mention; unfortunately, it is quite an uncomfortable item. Unlike rings, be they synchrotrons or storage rings, the optical functions α , β , and γ are not defined in a non-periodic

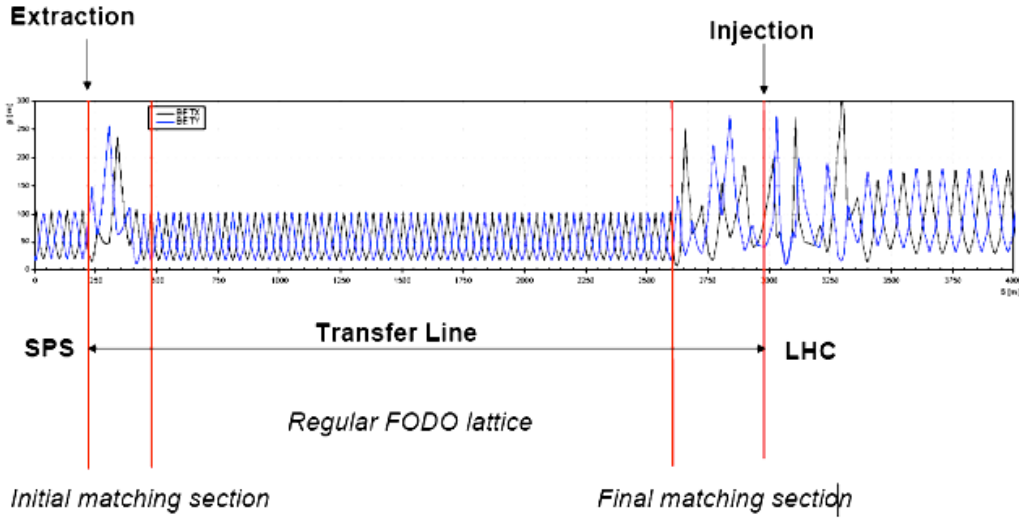


Fig. 25: Optics of the transfer line between the SPS and the HC



Fig. 26: The beam size must be measured at three locations in the transfer line

structure. Hill's equation (Eq. (28)) requires a periodic system and so does its solution. Still, this description is very powerful and so our colleagues from the non-periodic world love to use our language. However, we should be aware of this issue. In Eq. (60), we have learnt how to transform the optical functions from one position in the lattice to another, knowing the focusing elements in between. This means that if we know, e.g., the Twiss functions at the beginning of a transfer line, we can calculate them through the complete linear structure. An example is given in Fig. 25.

In the case of the example in Fig. 25, the optical functions at the beginning of the structure are defined, i.e., uniquely determined by the periodicity of the pre-accelerator, the SPS synchrotron. At the beginning and the end of the transfer line, special matching sections have been introduced to transform the periodic beta-functions from the SPS lattice onto the transfer line structure and from here to the LHC cells. Usually, such a matching section leads for a moment to a somehow increased beam amplitude (owing to the distorted beta-functions) and we have to take care to limit the aperture needs to reasonable values.

More complicated however is the case where a circular pre-accelerator does not exist. In such a case, we have to 'guess' the initial values of α , β , and γ , or, better, we have to measure them at the initial position before we can apply Eq. (60). To do so, we have to perform three measurements at three different locations in the line (see Fig. 26):

$$x(s) = a\sqrt{\beta(s)} \cos(\psi(s) - \phi)$$

$$x'(s) = a\sqrt{\beta(s)} (-\sin(\psi(s) - \phi))\psi' + \frac{\beta'(s)}{2\sqrt{\beta}} a \cos(\psi(s) - \phi)$$

Here we follow a beautiful explanation from Phil Bryant [10]; this is the way the trick goes.

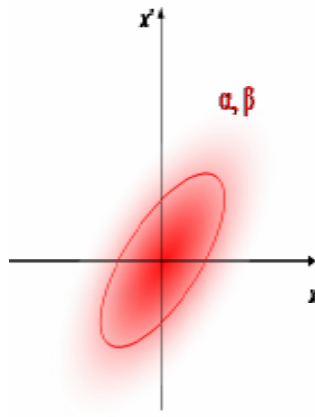


Fig. 27: Example of the transverse beam size measured in a transfer line

Assume that we measure the particle distribution, which might look like the example in Fig. 27.

Fitting a reasonable ellipse to the distribution, we can deduce the standard deviation of the, hopefully, nicely Gaussian-distributed particle density (... OK, for other than Gaussian distributions, it will also work more or less). So we obtain

$$\sigma = \sqrt{\varepsilon\beta} \quad (62)$$

and, as the beam emittance is constant, we can write—referring to each of the three positions s_0 , s_1 , and s_2 —

$$\varepsilon = \frac{\sigma_0^2}{\beta_0} = \frac{\sigma_1^2}{\beta_1} = \frac{\sigma_2^2}{\beta_2} \quad (63)$$

Now, from Eq. (61), we know how the beta-functions transform through the lattice and so we can express β_1 and β_2 as a function of the initial value β_0 :

$$\beta_1 = C_1^2\beta_0 - 2C_1S_1\alpha_0 + \frac{S_1^2}{\beta_0} (1 + \alpha_0^2) \quad (64)$$

$$\beta_2 = C_2^2\beta_0 - 2C_2S_2\alpha_0 + \frac{S_2^2}{\beta_0} (1 + \alpha_0^2) \quad (65)$$

Here, C_1 , S_1 , C_2 , and S_2 describe the matrix elements of the product matrix from point s_0 to s_1 and from s_0 to s_2 , respectively. Using this information, we can determine both α_0 and β_0 :

$$\alpha_0 = \frac{1}{2}\beta_0\Gamma, \quad (66)$$

$$\beta_0 = \frac{1}{\sqrt{\left(\frac{\sigma_1}{\sigma_0}\right)^2/S_1^2 - (C_1/S_1)^2 + (C_1/S_1)\Gamma - \Gamma^2/4}}, \quad (67)$$

where we introduced the parameter

$$\Gamma = \frac{(\sigma_2/\sigma_0)^2/S_2^2 - (\sigma_1/\sigma_0)^2/S_1^2 - (C_2/S_2)^2 + (C_1/S_1)^2}{C_1/S_1 - C_2/S_2},$$

et c'est ça.

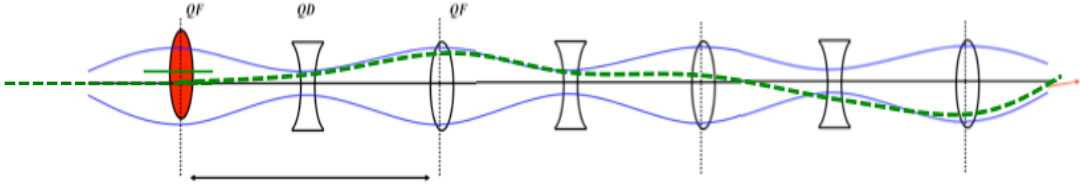


Fig. 28: Effect of a misaligned quadrupole in a transfer line. QD, defocusing quadrupole; QF, focusing quadrupole

6 Dipole errors and quadrupole misalignment

The design orbit, and thus the geometry of the ring or transfer line, is defined by the strength and arrangement of the dipole magnets. Under the influence of imperfections in the dipole field and (transverse) misalignment of the quadrupole magnets, unwanted deflection fields (‘kicks’) are created that influence this orbit. If these distortions are small enough (and hopefully they are), we will still obtain an orbit that is not too far away from the design. It is this ‘reference orbit’ that acts as a reference (hic) for the single-particle trajectories (i.e., the betatron oscillations) and we have to take care that it does not differ too much from the design.

A special issue, however, arises from the fact that in a ring this ‘reference orbit’ has, by definition, to be closed. While in a transfer line the effect of external distortions is somehow straightforward, in a periodic situation we have to be a bit more careful. For simplicity, we assume a small error and describe the effect as a sudden change of the particle’s angle x' ,

$$\Delta\theta = \Delta x' = \frac{dl}{\rho} = \frac{\int \delta B dl}{B\rho}, \quad (68)$$

where we have again normalized the field error by the beam rigidity to obtain the deflection angle x' .

In a misaligned quadrupole, we get exactly the same problem. An offset Δx in the presence of a field gradient g leads to an effective dipole field that deflects the beam:

$$\Delta\theta = \frac{\int \Delta B dl}{B\rho} = \frac{\int \Delta x g dl}{B\rho}. \quad (69)$$

For a transfer line, the resulting effect is trivial. Assuming a short, localized deflection, the amplitude of the particle is not affected by the field, but the angle x' is and so we can write:

$$x_f = x_i = 0, \quad (70)$$

$$x'_f = x'_i + \Delta x' = x'_i + \frac{\int \delta B dl}{B\rho}, \quad (71)$$

where the indices ‘i’ and ‘f’ refer to the position just in front of the kick and straight after. From this moment on, the originally ideal trajectory will be transformed through the lattice elements in the usual way:

$$\begin{pmatrix} x \\ x' \end{pmatrix}_s = \mathbf{M} \begin{pmatrix} x \\ x' \end{pmatrix}_0, \quad (72)$$

which is shown qualitatively for a transfer line in Fig. 28.

In a circular machine, things get a bit more complicated. As we talk about a ring, the periodic boundary conditions after one turn have to be taken into account. Mathematically, we express this fact by:

$$x(s+L) = x(s), \quad x'(s+L) + dx' = x'(s). \quad (73)$$

The kick creates an orbit deflection that travels (i.e., oscillates) around the complete ring and leads—unlike the situation in a transfer line—to an offset even at the origin of the kick itself, which is unchanged

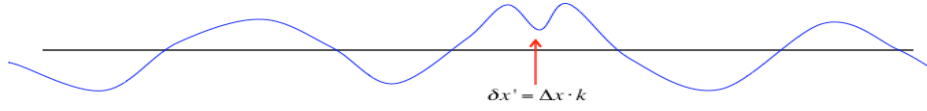


Fig. 29: Effect of a misaligned quadrupole in a ring: owing to the periodicity condition, the orbit has to close upon itself.

turn after turn; we still get a closed orbit. However, as the trajectory has to close upon itself, the angle x' after one turn has to take the distortion $\delta x'$ into account (Fig. 29).

Starting from the general solution of Hill's equation, and using the periodicity condition, we write for the amplitude:

$$x(s) = a\sqrt{\beta(s)} \cos(\psi(s) - \phi) \quad (74)$$

$$x(s+L) = x(s) \quad (75)$$

$$a\sqrt{\beta(s+L)} \cos(\psi(s) + 2\pi Q - \phi) = a\sqrt{\beta(s)} \cos(\psi(s) - \phi) \quad (76)$$

The amplitude factor a will be determined by the periodicity conditions and, clearly enough, the phase advance per turn increases by

$$\psi(s+L) = 2\pi Q .$$

As the amplitude function β is periodic, by definition, we obtain as a first condition:

$$\cos(2\pi Q - \phi) = \cos(-\phi) = \cos(\phi) , \quad (77)$$

$$\phi = \pi Q . \quad (78)$$

The boundary condition set by the amplitude fixes the initial condition for the phase ϕ . Following the same arguments, but now for the angle x' , we get

$$x(s) = a\sqrt{\beta(s)} \cos(\psi(s) - \phi) , \quad (79)$$

$$x'(s) = a\sqrt{\beta(s)} (-\sin(\psi(s) - \phi))\psi' + \frac{\beta'(s)}{2\sqrt{\beta}} a \cos(\psi(s) - \phi) , \quad (80)$$

and writing $\delta x'$ for the local kick due to the field distortion,

$$x'(s+L) + \delta x' = x'(s) ,$$

we get

$$\begin{aligned} -a \frac{1}{\sqrt{\beta(\tilde{s}+L)}} \sin(2\pi Q - \phi) + \frac{\beta'(\tilde{s}+L)}{2\beta(\tilde{s}+L)} \sqrt{\beta(\tilde{s}+L)} a \cos(2\pi Q - \phi) + \delta x' \\ = -a \frac{1}{\sqrt{\beta(\tilde{s})}} \sin(-\phi) + \frac{\beta'(\tilde{s})}{2\beta(\tilde{s})} \sqrt{\beta(\tilde{s})} a \cos(-\phi) . \end{aligned}$$

Here we have explicitly written \tilde{s} for the position of the dipole field error, to emphasize that, e.g., the optical functions are to be taken at this position. Knowing that, from the periodicity condition we derived,

$$\beta(s+L) = \beta(s), \quad \phi = \pi Q , \quad (81)$$

we can solve for the amplitude a and get

$$a = \delta x' \sqrt{\beta(\tilde{s})} \frac{1}{2 \sin(\pi Q)} . \quad (82)$$

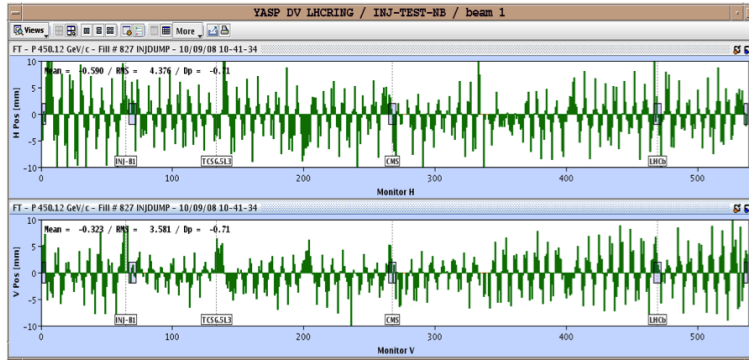


Fig. 30: Measured orbit in LHC during commissioning of the machine

Inserting this equation into Eq. 80, we get the final result that the amplitude of the closed orbit under the influence of a single dipole distortion (or quadrupole misalignment) is given by

$$x(s) = \delta x' \sqrt{\beta(\tilde{s})} \sqrt{\beta(s)} \frac{\cos(\psi(s) - \phi)}{2 \sin(\pi Q)}. \quad (83)$$

We conclude that the distorted orbit depends on the kick strength, the local β -function at the location \tilde{s} of the distortion, and the β -function at the observation point s . In addition, there is a resonance denominator, which will amplify any external orbit distortion, if the tune in the corresponding plane is on—or close to—an integer value. In such a case, the particle amplitude will increase ad infinitum and lead very quickly to particle losses; so better watch your tune!

For completeness: if we do not refer to a special starting point and express the orbit distortion as normalized dipole strength, $1/\rho(\tilde{s})$, we get the general expression

$$x(s) = \frac{\sqrt{\beta(s)}}{2 \sin(\pi Q)} \oint \sqrt{\beta(\tilde{s})} \frac{1}{\rho(\tilde{s})} \cos(|\psi(\tilde{s}) - \psi(s)| - \pi Q) d\tilde{s}. \quad (84)$$

We would not like to close this section without showing a real example of orbits for both cases, the closed orbit in a storage ring and the orbit in a transfer line or linacs. We have already seen an example of the first case in Fig. 11, which we plot here once more, for simplicity (Fig. 30). It shows the closed orbit of the LHC storage ring during the start-up phase of the machine, where considerable amplitudes in both planes were observed. The tune of the machine was set to $Q_x = 64.31$, so sufficiently away from resonance conditions. Still, the alignment tolerances of the magnets of $\Delta x \approx \Delta y \approx 150 \mu\text{m}$ caused a considerable orbit distortion of up to 10 mm.

The next plot, Fig. 31, refers to the situation in a transfer line (observed at the HERA collider at DESY). While in the first part of the structure the oscillations are well corrected and small, suddenly a strong trajectory fluctuation is created, owing to a misaligned quadrupole lens in the middle of the lattice. As the transfer line is not closed upon itself, the observed orbit develops according to Eqs. (71) and (72).

6.1 Emittance in electron rings or linacs

There is a special issue about electron beams that should not be forgotten: these particles are so light in weight (or, to be scientifically more correct, their Lorentz factor gamma is, even for moderate particle energies, already so large) that they emit radiation whenever accelerated or bent. This so-called synchrotron radiation has a strong influence on the beam dynamics, see, e.g., Ref. [11]. Summarizing these facts, we can state the following.

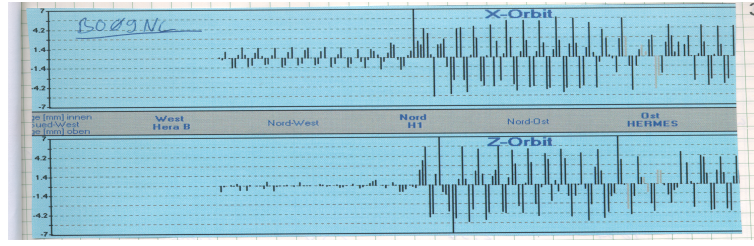


Fig. 31: Measured orbit in a beam transfer line, including the effect of a quadrupole lens that is misaligned in both planes.

- The power of the radiated synchrotron light depends on the energy of the particle ($\gamma = E/m_0c^2$) and the bending radius ρ of the trajectory under the influence of the field acting on it,

$$\Delta P = \frac{e^2 c}{6\pi\epsilon_0} \frac{\gamma^4}{\rho^2} . \quad (85)$$

- The energy loss per turn in a circular machine is given by

$$\Delta E = \frac{e^2}{3\epsilon_0} \frac{\gamma^4}{\rho} . \quad (86)$$

- The critical energy $E_{\text{crit}} = \hbar * \omega$ of the emitted radiation is given by

$$\omega_c = \frac{3c}{2} \frac{\gamma^3}{\rho} . \quad (87)$$

The damping effect of the light emission and the quantum effect of the emitted photons leads to an equilibrium emittance of the beam that is given by

$$\epsilon_{x_0} = \frac{C_q E^2}{J_0} \frac{\langle H \rangle_{\text{mag}}}{\rho} , \quad (88)$$

where J_x is the so-called damping partition number, which is determined by the lattice and is usually close to $J_x = 1$. The H -function describes the influence of the optical parameters α, β , and γ and dispersion D :

$$\langle H \rangle = \gamma D^2 + 2\alpha D D' + \beta D'^2 ; \quad (89)$$

C_q is a constant that we usually introduce to make our equations more compact. It is given by

$$C_q = \frac{55}{32\sqrt{3}} \frac{\hbar c}{(m_e c^2)^3} \quad (90)$$

and for electrons it has the numerical value

$$C_q = 1.468 \times 10^{-6} \left[\frac{\text{m}}{\text{GeV}^2} \right] . \quad (91)$$

Now, while this clearly has a strong impact on the magnet strength and the design of the lattice, it also affects the orbit correction scheme. Any (!) external field, including off-centre quadrupoles, and including the effect of orbit corrector dipoles, will influence the beam emittance. In the quest for the highest brilliance of the emitted light and so for smallest possible beam emittances, therefore, these effects must be taken into account.

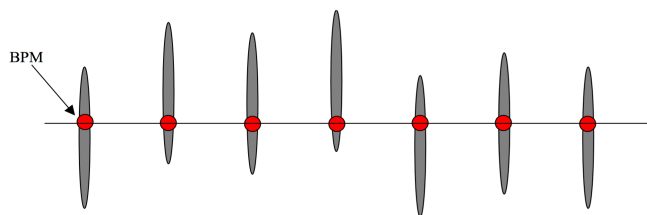


Fig. 32: Lattice with misaligned quadrupoles and perfect beam position monitors (BPMs)

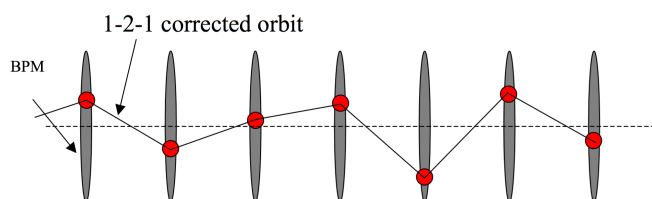


Fig. 33: Lattice with perfectly aligned quadrupoles but offsets in the reading of the beam position monitors (BPMs). While the actual orbit is perfect, the beam position monitor readings simulate an orbit distortion.

Any deflecting field will change (i.e. create) additional beam emittance and we have to be careful when it comes to orbit corrections. Assume the two extreme cases, which are shown schematically in Figs. 32 and 33.

In the case of Fig. 32, an orbit correction algorithm will tell us exactly what to do. Each misaligned quadrupole will lead to an orbit deflection, which can and should be corrected by the corrector dipole next to it. The result will be a nearly perfect compensation of the quadrupole offsets and a nicely small beam emittance.

Consider, however, the case of Fig. 33. Here, the quadrupoles are perfectly aligned and it is the beam position monitor system that causes the trouble. Nobody is perfect and so even beam position monitors can have some reading errors that lead to artificial beam position offsets. A straightforward approach, as explained, will reduce the beam position monitor readings, but in reality lead to a distorted orbit and so create additional dispersion in the machine and lead to increased emittances. Especially in the vertical plane this effect is most serious, as vertical bending fields will not usually be present in the machine and the emittance in this plane should be minimized. Special techniques are needed and have been developed to avoid such a problem. Dispersion-free steering methods are widely used [12, 13]; instead of correcting the orbit (i.e., the beam position monitor readings), we concentrate directly on the dispersion that can be measured in the machine and we power our corrector magnets in such a way that the dispersion is minimized around the storage ring.

In the commissioning phase of an accelerator, and during daily operation, such orbit oscillations should be reduced as much as possible. At first sight, they eat up free aperture and can easily lead to particle losses at the vacuum chamber wall. Beyond that, the beam will be off-centre in the magnet elements and especially in the presence of sextupole magnets; this will create optics problems (tune shift and beta beat) and, in the case of vertical offsets, will create coupling. Talking for a moment again about electron beams, any offset in a magnetic field of a quadrupole or higher-order magnet will immediately create synchrotron radiation and unwanted spurious dispersion with its serious drawback for the beam emittance. In light sources and modern lepton colliders, where we seek for the smallest vertical emittance,

any vertical deflecting fields should be avoided; here, people use a series of orbit correction tools that are powered ‘on-beam’ in feedback loops to keep the orbit as ‘golden’ as possible.

Moreover, during the actual injection or extraction process, the effect of steering errors, as well as the effect of optics mismatch, will lead to emittance growth that can be large enough to spoil the beam quality. A summary of these problems and their impact on the beam is actually the topic of this school and will be presented in several of the next papers of these proceedings.

7 Conclusion

The topic of injection, extraction, and beam transfer is one of the most critical issues in the lifetime of a particle beam, and therefore in the design of an accelerator complex. The fast-changing fields of the lattice elements involved usually represent non-adiabatic changes that—if handled in an improper way—can easily destroy the beam quality. A decent optimization of the design and the quality of the hardware involved, and the possibility of measuring the relevant beam parameters (and optimizing them accordingly), is a must. The optimization of a typical beam injection, e.g., will therefore involve a careful steering of the orbit amplitude and angle in both transverse planes, matching of the optics (horizontal and vertical α and β functions), and their measurement. Similar care has to be taken in the longitudinal plane, which will be discussed in another paper. Here, we have to optimize and control the bunch length and the phase and the energy of the injected particle bunches.

This can be tedious work, but it pays off as soon as it comes to beam quality, background reduction, emittance dilution, and, for a collider, finally, the luminosity that we can get out of the machine.

And so, in the end, and after all, we want to conclude this brief paper with a word of consolation:

Usually it works.

References

- [1] K. Wille, *The Physics of Particle Accelerators* (Oxford University Press, Oxford, 2000).
- [2] J. Rossbach and P. Schmüser, Basic course on accelerator optics, edited by S. Turner, CERN-1994-001, (CERN, Geneva, 1994), pp. 17–88, <http://dx.doi.org/10.5170/CERN-1994-001.17>
- [3] B.J. Holzer, Lattice design in high-energy particle accelerators, edited by W. Herr, CERN-2014-009, (CERN, Geneva, 2014).
- [4] E. Jaeschke *et al.*, The Heidelberg test storage ring for heavy ions TSR, Proc. EPAC, Rome, 1988, edited by S. Tazzari (World Scientific, Teaneck, 1988), p. 365.
- [5] H. Goldstein, *Klassische Mechanik* (Akademische Verlag-Gesellschaft, Wiesbaden, 1981).
- [6] A. Wolski, *Beam Dynamics in High Energy Particle Accelerators* (Imperial College Press, London, 2014), p. 59.
- [7] HERA Design Team, HERA: a proposal for a large electron proton colliding beam facility at DESY, DESY-HERA-81/10 (DESY, Hamburg, 1981).
- [8] E.D. Courant and H.S. Snyder, *Ann. Phys.* **6** (1958) 1.
- [9] W. Shakespeare, *Henry V*, Act 3, Scene 1, Line 1.
- [10] P.J. Bryant, Proc. CAS–CERN Accelerator School, 5th General Accelerator Physics Course, Jyväskylä, Finland, 1992, CERN-1994-001 (CERN, Geneva, 1994), pp. 17–88. <http://dx.doi.org/10.5170/CERN-1994-001.17>
- [11] L. Rivkin, these proceedings
- [12] T.O. Raubenheimer and R.D. Ruth, *Nucl. Instrum. Methods* **A302** (1991) 191.
- [13] R. Assmann *et al.*, Emittance optimization with dispersion free steering at LEP, CERN-SL-2000-078-OP, (CERN, Geneva, 2000).

Bibliography

- B.J. Holzer, Proc. CAS–CERN Accelerator School, Course on Superconductivity for Accelerators, Erice, Italy, 2013, CERN-2014-005
- F. Tecker, Longitudinal beam dynamics, in Proceedings of the CAS-CERN Accelerator School: Advanced Accelerator Physics Course, Trondheim, Norway, 18–29 August 2013, edited by W. Herr, CERN-2014-009 (CERN, Geneva, 2014), p. 1–21, <https://doi.org/10.5170/CERN-2014-009.1>.
- C. Bernardini, *Phys. Persp.* **6** (2004) 156.
- LHC design report, CERN-2004-003 (CERN, Geneva, 2004), <https://doi.org/10.5170/CERN-2004-003-V-1>, <https://doi.org/10.5170/CERN-2004-003-V-2>, <https://doi.org/10.5170/CERN-2004-003-V-3>.
- P.J. Bryant, A brief history and review of accelerators, in Proceedings of the CAS-CERN Accelerator School: 5th General Accelerator Physics Course, Jyväskylä, Finland, 7–18 September 1992, edited by S. Turner, CERN-1994-001 (CERN, Geneva, 1994), p. 1-16, <https://doi.org/10.5170/CERN-1994-001.1>.
- N. Walker, Emittance preservation, CAS–CERN Accelerator School, 5th Intermediate Accelerator Physics Course, Daresbury, UK, 2007.